

PETA: Evaluating the Impact of Protein Transfer Learning with Sub-word Tokenization on Downstream Applications

Yang Tan^{†a,b} (tyang@mail.ecust.edu.cn), Mingchen Li^{†a,b} (lmc@mail.ecust.edu.cn), Pan Tan^{b,c} (tanpan@pjlab.org.cn), Ziyi Zhou^c (zy-zhou@sjtu.edu.cn), Huiqun Yu^{*a} (yhq@ecust.edu.cn), Guisheng Fan^{*a} (gsfan@ecust.edu.cn), Liang Hong^{*b,c} (hongl3liang@sjtu.edu.cn)

^a School of Information Science and Engineering, East China University of Science and Technology, Shanghai 200240, China

^b Shanghai Artificial Intelligence Laboratory, Shanghai 200240, China

^c Shanghai National Center for Applied Mathematics (SJTU Center), & Institute of Natural Sciences, Shanghai Jiao Tong University

Corresponding Author:

Huiqun Yu

School of Information Science and Engineering, East China University of Science and Technology, Shanghai 200240, China

Email: yhq@ecust.edu.cn

Corresponding Author:

Guisheng Fan

School of Information Science and Engineering, East China University of Science and Technology, Shanghai 200240, China

Email: gsfan@ecust.edu.cn

Corresponding Author:

Liang Hong

Shanghai Artificial Intelligence Laboratory, Shanghai 200240, China
Shanghai National Center for Applied Mathematics (SJTU Center), & Institute of
Natural Sciences, Shanghai Jiao Tong University
Email: hongl3liang@sjtu.edu.cn

PETA: Evaluating the Impact of Protein Transfer Learning with Sub-word Tokenization on Downstream Applications

Yang Tan^{†a,b}, Mingchen Li^{†a,b}, Pan Tan^{b,c}, Ziyi Zhou^c, Huiqun Yu^{a,*},
Guisheng Fan^{a,*}, Liang Hong^{b,c,*}

^a*School of Information Science and Engineering, East China University of Science and Technology, Shanghai 200240, China*

^b*Shanghai Artificial Intelligence Laboratory, Shanghai 200240, China*

^c*Shanghai National Center for Applied Mathematics (SJTU Center), & Institute of Natural Sciences, Shanghai Jiao Tong University*

Abstract

Large protein language models are adept at capturing the underlying evolutionary information in primary structures, offering significant practical value for protein engineering. Compared to natural language models, protein amino acid sequences have a smaller data volume and a limited combinatorial space. Choosing an appropriate vocabulary size to optimize the pre-trained model is a pivotal issue. Moreover, despite the wealth of benchmarks and studies in the natural language community, there remains a lack of a comprehensive benchmark for systematically evaluating protein language model quality. Given these challenges, PETA trained language models with 14 different vocabulary sizes under three tokenization methods. It conducted thousands of tests on 33 diverse downstream datasets to assess the models' transfer learning capabilities, incorporating two classification heads and three random seeds to mitigate potential biases. Extensive experiments indicate that vocabulary sizes between 50 and 200 optimize the model, whereas sizes exceeding 800 detrimentally af-

*Corresponding author.

Email addresses: tyang@mail.ecust.edu.cn (Yang Tan[†]), lmc@mail.ecust.edu.cn (Mingchen Li[†]), tanpan@pjlab.org.cn (Pan Tan), zy-zhou@sjtu.edu.cn (Ziyi Zhou), yhq@ecust.edu.cn (Huiqun Yu), gsfan@ecust.edu.cn (Guisheng Fan), hongl3liang@sjtu.edu.cn (Liang Hong)

[†]: Yang Tan and Mingchen Li are co-first authors.

fect the model’s representational performance. Our code, model weights and datasets are available at <https://github.com/ginmm/ProteinPretraining>.

Keywords: Pre-training protein language model, Amino acid tokenization, Vocabulary size, Evaluation benchmark

1. Introduction

Naturally occurring proteins play a pivotal role in sustaining life forms and have found extensive applications in human endeavors, including gene editing (Doudna & Charpentier, 2014; Hsu et al., 2014), drug discovery (Scott et al., 2016), and enzymatic catalysis (Lee, 2006). Furthermore, gaining insights into protein properties or enhancing their functionality holds significant practical value, such as enhancing the function of the original protein (Joo et al., 1999) or annotating an unknown sequence (Sharan et al., 2007). Protein engineering typically follows two common approaches: laboratory-based experiments and computation-based methods. The former includes structural analysis (Feng et al., 2014), expression purification (Lesley, 2001) and direct evolution (Arnold, 1998), while valuable, are time-consuming and heavily reliant on domain-specific knowledge. This limitation falls short of meeting the evolving demands of both the scientific community and industry. Conversely, the computation-based modeling strategy relies on machine-learning or physics-based methods that are often not particularly accurate but are cost-effective and time-saving. Thanks to the advancements in protein sequencing technology (Ma, 2015), new avenues have opened up for training large-scale protein models capable of capturing a more comprehensive understanding. For instance, Meta has introduced ESM series (Lin et al., 2023; Meier et al., 2021; Rives et al., 2021) to leverage the UniProt database (Consortium, 2019) which contains over 200 million protein sequences or its subsets for training purposes.

A plethora of machine-learning methods have been developed to address various protein-related tasks. Protein representation learning primarily employs two main strategies. The first strategy, recognizing the significance of pro-

tein structures in functional determination, employs structure-aware encoders trained with implicit topological constraints. Notable examples include ESM-GearNet (Zhang et al., 2023) and LM-GVP (Wang et al., 2022). However, residue-level structural models often exhibit inferior performance compared to protein language models (PLMs) across most tasks (Zhang et al., 2022). These methods, in contrast to PLMs, tend to focus on a limited and biased subset of the Protein Data Bank (PDB) (Berman et al., 2000), limiting their training data scope and generalization capabilities. While efforts have been made to expand the training dataset scale, such as incorporating AlphaFold database (Varadi et al., 2022) data in some work (Hsu et al., 2022; Zhang et al., 2023), their parameters and data sizes still remain relatively small in comparison to language models.

The second strategy involves protein language processing, a well-established approach that models the inherent connections within protein sequences and effectively captures co-evolutionary information. Various works have harnessed different sequence encoders or decoders in this strategy, including Convolutional Neural Networks (CNNs) (Yang et al., 2022a), Long Short-Term Memory networks (LSTMs) (Alley et al., 2019; Rao et al., 2019), BERT models (Lin et al., 2023; Meier et al., 2021; Rives et al., 2021), Generative Pre-trained Transformers (GPTs) (Madani et al., 2023; Nijkamp et al., 2022; Ferruz et al., 2022), and Transformers (Elnaggar et al., 2021, 2023). Protein language models have demonstrated outstanding performance across a wide range of tasks and constitute a primary focus of this paper.

Nonetheless, there is still a lack of comprehensive analysis of how amino acid combinations influence language models, it’s a fundamental and significant issue in language model training (Rust et al., 2020; Choo & Kim, 2023) that has thus far been overlooked in the protein area. In this paper, we draw inspiration from Asgari et al. (2019) and aim to develop a universal amino acid coding approach capable of delivering robust performance across various protein-related tasks, while harnessing the benefits of knowledge sharing and transfer as shown in Fig 1. To facilitate a thorough assessment and take cues from the

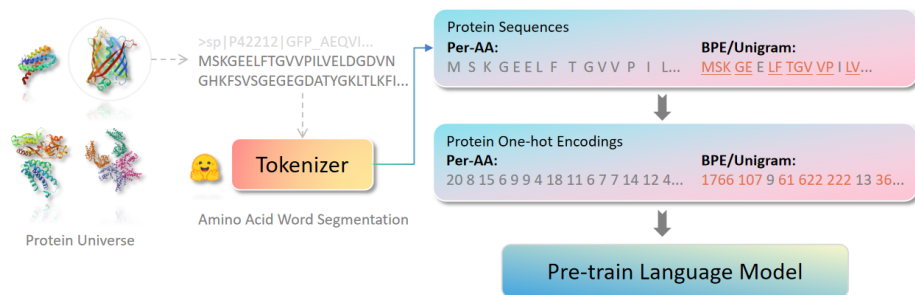


Figure 1: The protein sequence is formed into a new discrete token sequence through different word segmentation methods. As the size of the vocabulary increases, the amino acid composition of a single token becomes more complex.

success of benchmark datasets in domains like computer vision and natural language processing, e.g., ImageNet (Deng et al., 2009) and GLUE (Wang et al., 2018), we have meticulously curated a collection of 33 datasets categorized into 15 distinct tasks. These datasets are integral to advancing the realm of deep learning in protein comprehension. Our PETA benchmark encompasses five groups, covering tasks in protein fitness prediction, protein localization prediction, protein-protein interaction prediction, protein solubility prediction, and protein structure prediction. For each individual dataset, we evaluate the performance of three types of tokenizers, two new residue-pair tokenizers are used to train five models with distinct vocabularies respectively and one per-amino acid (Per-AA) model acts as baseline. Two different pooling mechanisms and three random seeds are employed in downstream tasks to mitigate potential classification biases. We anticipate that our comprehensive analysis of protein tokenizers and the PETA benchmark will serve as a pivotal milestone for the continued advancement of protein language model pre-training.

Our contributions are as follows:

- **Protein Tokenization Analysis:** We summarize how the amino acid coding approach enhances the effectiveness of protein language models across diverse protein-related tasks. By addressing the influence of amino

acid combinations, the research offers valuable insights into the optimization of protein language models.

- **Creation of the PETA Benchmark:** We meticulously curate the PETA benchmark, a comprehensive collection of 33 datasets categorized into 15 distinct protein-related tasks. This benchmark spans 5 diverse aspects of protein research. It provides a standardized evaluation framework for protein language models.
- **Comprehensive Experiments:** We have conducted thousands of experimental evaluations to ensure the validity of the results, and the model weights, code, etc. are completely open source in the community.

2. Related work

2.1. Protein Representation Learning

Representation learning harnesses knowledge acquired from large-scale corpora to generalize across various tasks. Early approaches primarily employed machine learning techniques from natural language processing, such as word2vec (Mikolov et al., 2013) and doc2vec (Le & Mikolov, 2014), to extract features from protein sequences (Wang et al., 2017; Mejía-Guerra & Buckler, 2019; Wan & Zeng, 2016). Recently, deep learning has exhibited tremendous potential by enabling models with increased capacity and deeper encoders, capable of handling millions or billions of protein sequences. ESM-1V (Meier et al., 2021), SESNet (Li et al., 2023), and ECNet (Luo et al., 2021), which focus on predicting mutation fitness. Additionally, Meta’s ESM-1b (Rives et al., 2021) and ESM-2 (Lin et al., 2023) employ mask language modeling. ProtTrans (Elnaggar et al., 2021) pre-trains language models under various architectures (Lan et al., 2019; Devlin et al., 2018; Vaswani et al., 2017; Raffel et al., 2020; Ye et al., 2020), while XTrimo (Chen et al., 2023) aligns its pre-trained architecture with GLM (Du et al., 2021). Ankn (Elnaggar et al., 2023) uses an asymmetric encoder and decoder framework and different mask probabilities to improve the pre-training

performance. CPCProt (Lu et al., 2020) leverages a contrastive predictive coding loss, whereas ProGen (Madani et al., 2023; Nijkamp et al., 2022), UniRep (Alley et al., 2019), ProXLNet (Elnaggar et al., 2021), ProtGPT2 (Ferruz et al., 2022), and Tranception (Notin et al., 2022) are pre-trained using next amino acid prediction tasks. Although many of these approaches share common objectives with natural language processing, there are also innovations like CARP (Yang et al., 2022a) which employ convolutional networks for downstream tasks. Some works delve into protein multiple sequence alignments (MSAs) (Rao et al., 2021; Biswas et al., 2021; Notin et al., 2022), while others take structure-based approaches to extract topology information for inverse folding (Hsu et al., 2022; Yang et al., 2022b; Jing et al., 2020) or protein design (Dauparas et al., 2022; Zheng et al., 2023). Notably, LM-GVP (Wang et al., 2022) and MIF-ST (Yang et al., 2022b) integrate sequence and structural information to enhance the learning of effective protein representations. In this benchmark, our primary focus revolves around evaluating the performance of language models utilizing different tokenization strategies.

2.2. Protein Modeling Benchmarks

A comprehensive benchmark has shown great influence in the traditional computer science community and driven the research direction of different works (Wang et al., 2018, 2019; Lin et al., 2014; Deng et al., 2009; Kay et al., 2017). However, it is worth noting that the field of computing protein engineering still lacks a large-scale benchmarking framework. In contrast, the biennial Critical Assessment of Protein Structure Prediction (CASP) (Kryshtafovych et al., 2021) has emerged as a gold standard for assessing advancements in protein structure prediction. In tandem with CASP, the Critical Assessment of Functional Annotation (CAFA) challenge (Zhou et al., 2019) has been established to evaluate the prediction of protein functions. Several notable works, such as DeepSequence (Riesselman et al., 2018), Envision (Gray et al., 2018), and ProteinGym (Notin et al., 2022), focus on measuring very different functional fitness variations in response to diverse protein modifications, including substitutions and

insertions/deletions. Techniques like deep mutational scanning (DMS) (Fowler & Fields, 2014) and other protein engineering methods are used to build up these datasets. On the other hand, works like SoluProtMutDB (Velecký et al., 2022), SKEMPI (Moal & Fernández-Recio, 2012), and ProThermDB (Nikam et al., 2021) concentrate on assessing specific properties concerning single amino acid variations (SAVs). Additionally, FLIP (Dallago et al., 2021) offers various data partitioning methods across three protein landscapes for evaluating fitness prediction. The TAPE benchmark (Rao et al., 2019) encompasses five tasks, with three focusing on structure prediction and the remaining two targeting fitness prediction. PEER (Xu et al., 2022) encompasses seventeen biologically relevant tasks spanning five aspects of protein understanding. ProteinGLUE (Capel et al., 2022) comprises seven downstream tasks designed for self-supervised protein representation learning. DeepLoc (Almagro Armenteros et al., 2017; Thumhuri et al., 2022) provides datasets for subcellular localization classification. The STRING database (Szklarczyk et al., 2016) annotates protein-protein interactions (PPIs) with seven types of interactions. TDA (Huang et al., 2021) generates protein-related datasets and tasks tailored for drug discovery. ESOL website (Niwa et al., 2009) aggregates solubility scores for ensemble E.coli proteins.

3. PTEA

We designed PETA to answer two important questions:

- Is residue-wise tokenizer good enough for protein language model pre-training?
- How do different vocab sizes influence the representation ability on downstream tasks?

Most of the works choose one tokenizer aligned with previous research without much concern, to answer the first question, we utilize three amino acid segmentation strategies including residue-wise and sub-word tokenizer. For the

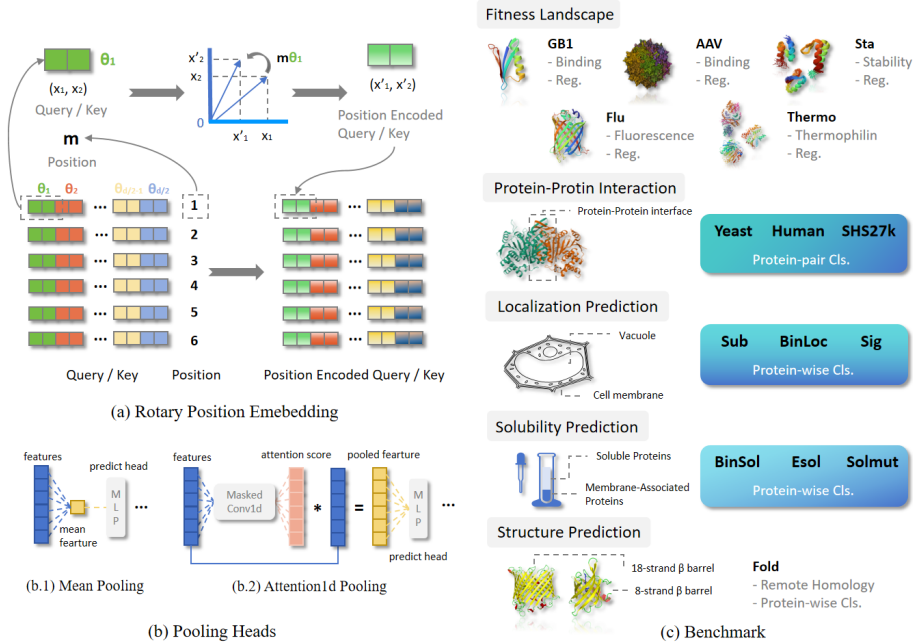


Figure 2: The framework of PETA. (a) Pre-trained models use rotary position embedding, which possesses favorable theoretical properties and is an absolute positional encoding applicable to linear Attention. (b) We employed two distinct classification heads, namely mean pooling and attention1d pooling. The former is the most commonly used method at present, while the latter is relatively more complex. (c) Our benchmark comprises 15 downstream tasks, which can be categorized into five groups. Some of these downstream tasks include multiple datasets or data splitting methods, amounting to a total of 33 datasets.

second question, we design vocab size from $\{50, 100, 200, 800, 1600, 3200\}$ for the Unigram and BPE segmentation method. The model trained under per-AA is the baseline, it has a vocabulary size of 33 and many works adopt this. In general, we utilize three tokenize methods, two types of classification heads and two model pipelines to solve different tasks in the PETA benchmark. The framework of PETA is shown in Fig 2.

3.1. Amino Acid Segmentation

In this study, we utilize three classic protein sequence segmentation methods: per-amino-acid encoding (Per-AA), byte pair encoding (BPE) (Gage, 1994), and unigram language modeling (Unigram) (Bengio et al., 2000) as shown in Fig 1. Per-AA focuses on individual amino acid units, enabling high-resolution analysis of subtle variations. BPE offers flexibility by segmenting sequences into subunits, effectively capturing structural information, while Unigram, based on character-level statistics, captures global sequence characteristics. These diverse methods collectively enhance our comprehensive analysis of protein sequences, each serving a unique role in addressing specific analytical requirements.

3.2. Pre-training Protein Language Models

3.2.1. Model Architecture

Our pre-training architecture employs RoFormer (Su et al., 2021), an autoencoding model that adopts a BERT-like structure augmented with rotary positional embeddings, as illustrated in Figure 2 (a). These rotary positional embeddings effectively harness positional information within sequences. Detailed hyperparameter configurations are delineated in the subsequent section. Initially, protein sequences are tokenized and transformed into one-hot encoded representations. These representations are subsequently fed into RoFormer’s encoder, which generates sets of hidden states that maintain the length consistency with the input tokenized sequence. Finally, these hidden states are transformed into a vector with a dimensionality corresponding to the vocabulary size, upon which a softmax function is applied to yield the reconstruction probability density distribution.

3.2.2. Pre-training Objective

We employ the masked language modeling (MLM) objective for pre-training our models (Lan et al., 2019). Given an input sequence, a subset of tokens is selected at random and replaced with a special mask token. The model is then

trained to predict these masked tokens based on the unmasked context tokens. The loss function for this objective can be defined as:

$$L_{MLM} = E_{x \sim X} E_M \sum_x -\log p(x_i | x_{/M}) \quad (1)$$

Here, x is a sequence from the dataset X , and $x_{/M}$ represents the sequence with masked tokens removed. $p(x_i | x_{/M})$ is the conditional probability of predicting the correct token x_i given the context $x_{/M}$. The aim is to minimize the negative log-likelihood of the true token at each masked index i , which in this case are amino acids, given the unmasked sequence as context. Intuitively, the model must learn to identify the dependencies between the masked and unmasked tokens to successfully predict the masked positions.

3.2.3. Language Modeling Evaluation Metrics

We use *Perplexity* to evaluate the performance of the masked language modeling, computed as:

$$Perplexity = \exp\left(-\frac{1}{N} \sum_{i=1}^N \log p(x_i | x)\right) \quad (2)$$

, where N is the number of validation sequences, as well as x_i is the i_{th} sequence of validation set. To account for potential unfair comparisons arising due to varying vocabulary sizes across different models, we introduce the metric of *Normalized Perplexity*. The formula for Normalized Perplexity is as follows:

$$Perplexity = \exp\left(-\frac{1}{N \times V} \sum_{i=1}^N \log p(x_i | x)\right) \quad (3)$$

, where V is the vocab size.

3.2.4. Pre-training Data

We train all models on UniRef90 (Suzek et al., 2015), a comprehensive protein sequence database that contains approximately 138 billion sequences from diverse life forms. This large-scale database serves as a robust training set for capturing the underlying patterns and intricacies associated with protein sequences. For model validation, a subset of 100,000 sequences is reserved from

the UniRef90 database. This validation set is instrumental in evaluating the generalization capability of the language models on unseen data. This setup ensures that the trained models are subjected to a variety of sequence patterns, thereby facilitating a more robust understanding of protein sequences. By reserving a significant number of sequences for validation, we also ensure an unbiased assessment of the model performance.

3.3. Classification Head

To avoid the potential bias caused by different classification methods, the *Mean Pooling* and *Attention1d Pooling* are adopted under our evaluation, as shown in Fig 2 (b). The former is trained on the average of features aligned with the first dimension, MLP and Relu activation are used to make a prediction. The latter is trained on an attention machine and 1D convolution layer to map different weights to embed and predict the label.

3.4. Model Pipeline

Protein-wise tasks. Learning a function $y = f_{\theta}(x)$ that maps protein x to the label y , where f_{θ} is parameterized by a sequence-based encoder and a classification head defined upon the residue-wise or residue-pair protein embedding.

Protein-pair tasks. Learning a function $y = f_{\theta}(x)$ that maps a pair of proteins (x, x') to the label y , where f_{θ} is parameterized by a pair of siamese sequence-based encoders and a classifier defined upon the sum of the embeddings of two proteins.

4. Benchmark Tasks

The PETA benchmark includes 15 tasks within 5 groups and 33 datasets in total, mainly focusing on protein-wise and protein-pair tasks. We have curated tasks from influential protein engineering applications and made updates to certain datasets to ensure their relevance and accuracy, a summary of the downstream dataset statistics is shown in Table 1.

Task Name	Task Category	Count	Source	Metric
Fitness Prediction				
GB1 fitness prediction (GB1)	Protein-wise Reg.	5	FLIP	Spearman
AAV fitness prediction (AAV)	Protein-wise Reg.	7	FLIP	Spearman
Thermostability prediction (Thermo)	Protein-wise Reg.	3	FLIP	Spearman
Fluorescence prediction (Flu)	Protein-wise Reg.	1	TAPE	Spearman
Stability prediction (Sta)	Protein-wise Reg.	1	TAPE	Spearman
Protein-Protein Interaction Prediction				
Yeast PPI prediction (Yeast)	Protein-pair Cls.	1	PETA	Accuracy
Human PPI prediction (Human)	Protein-pair Cls.	1	PETA	Accuracy
SHS PPI prediction (SHS27k)	Protein-pair Cls.	1	PETA	Accuracy
Localization Prediction				
Subcellular localization prediction (Sub)	Protein-wise Cls.	3	pro-loc, DeepLoc-2	Accuracy
Binary localization prediction (BinLoc)	Protein-wise Cls.	1	pro-loc	Accuracy
Sorting signal prediction (Sig)	Protein-wise Cls.	1	DeepLoc-2	Accuracy
Solubility Prediction				
Binary solubility prediction (BinSol)	Protein-wise Cls.	1	DeepSol	Accuracy
E.coli solubility prediction (Esol)	Protein-wise Reg.	1	GraphSol	MSE
Mutation solubility prediction (Solmut)	Protein-wise Reg.	3	PETA	Spearman
Structure Prediction				
Fold Prediction (Fold)	Protein-wise Cls.	3	TAPE	Accuracy

Table 1: Benchmark task details. Each task, along with its task name, category, the count of datasets, the source of dataset and evaluation metric are shown below. *Abbr.*, Reg.: regression; Cls.: classification; MSE: mean square error.

4.1. Fitness Prediction

This set of tasks aims to forecast functional attributes of proteins, which may be either discrete or continuous in nature.

GB1 fitness prediction assesses fitness scores among mutations within the GB1 landscape from Wu et al. (2016). Given a protein sequence x , we map it to a regression value $y \in \mathbb{R}$, where a fitness score of 1 represents the wild-type and 0 indicates non-binding affinity. In our analysis, we utilize all the dataset splits proposed in FLIP (Dallago et al., 2021), encompassing "one-vs-rest", "two-vs-rest", "three-vs-rest", "low-vs-high" and "Sampled".

Impact: GB1 serves as the binding domain of protein G (McCallister et al., 2000), an immunoglobulin binding protein found in Streptococcal bacteria (Sauer-Eriksson et al., 1995). This task stands as a gold standard for investigating epistatic interactions.

AAV fitness prediction entails the evaluation of fitness values associated with Adeno-associated virus (AAV) capsid proteins (Girod et al., 2002). Given a protein sequence x , we establish a mapping to a regression value $y \in \mathbb{R}$, focusing on the mutational window spanning positions 561 to 588 from Bryant et al. (2021). We adopt all the dataset splits from FLIP (Dallago et al., 2021), which includes "Mut-Des", "Des-Mut", "one-vs-rest", "two-vs-rest", "seven-vs-rest", "low-vs-high" and "Sampled".

Impact: AAV proteins are responsible for facilitating the integration of a DNA payload into a target cell by the virus (Vandenberghe et al., 2009). This task specifically addresses the prediction of fitness for an extended sequence subjected to mutations at select positions.

Thermostability prediction involves the analysis of protein melting curves, which are acquired through a mass spectrometry-based assay and meticulously sourced from Jarzab et al. (2020). In this endeavor, we focus on a protein sequence x , which is drawn from a vast pool of 48,000 proteins spanning 13 diverse species. Our objective is to predict a thermostability score $y \in \mathbb{R}$. For this analysis, we have employed the dataset splitting strategies "Human", "mixed_split", and "Human_cell" as outlined in FLIP (Dallago et al., 2021).

Impact: Thermostable proteins (Yeoman et al., 2010; Haki & Rakshit, 2003) demonstrate an ability to endure higher temperature conditions for extended periods or function at an accelerated rate. This task aligns closely with applications in protein engineering, particularly within industrial settings, where the enhanced stability of proteins can yield substantial benefits.

Fluorescence prediction primarily focuses on forecasting the fitness of mutants of the green fluorescent protein (GFP) (Labas et al., 2002), as documented by Sarkisyan et al. (2016). In this context, we are presented with a GFP mutant sequence x and aim to predict the corresponding fluorescence intensity $y \in \mathbb{R}$. We leverage the dataset and split methodology derived from TAPE (Rao et al., 2019), which involves training the model on lower-order mutants and subsequently evaluating it on higher-order mutants.

Impact: Green fluorescent protein can mark particular proteins in an organic structure by its green fluorescence (Willig et al., 2006), this makes it easier for researchers to observe. This task bears significance in uncovering mutational patterns that either enhance or diminish such vital biological properties.

Stability prediction endeavors to assess the resilience of proteins within their natural environment. It involves taking a protein sequence, denoted as x , and predicting its corresponding experimental stability score, denoted as $y \in \mathbb{R}$. In this pursuit, we leverage the dataset curated from (Rocklin et al., 2017) and employ the partitioning method introduced in TAPE (Rao et al., 2019). The training dataset comprises proteins sourced from four rounds of experimental design, while the test dataset encompasses proteins that are Hamming distance-1 neighbors of the top candidate proteins.

Impact: The design of stable proteins in the face of mutations plays a pivotal role in the field of protein engineering (Shoichet et al., 1995). This work is instrumental in various applications, such as ensuring the effective delivery of drugs before they degrade.

4.2. Protein-Protein interaction Prediction

Predicting protein-protein interactions (PPI) is pivotal for deciphering the intricate molecular networks underpinning cellular functions and disease mechanisms, guiding targeted therapeutic interventions.

Yeast PPI prediction involves the prediction of whether two yeast proteins interact with each other. When presented with two proteins, denoted as x_1 and x_2 from yeast, the classifier assigns a binary label $y \in 0, 1$ to signify the presence or absence of interaction between them. To accomplish this task, we utilize the yeast PPI dataset sourced from Guo et al. (2008). In this dataset, half of the instances represent positive cases, selected from the DIP_20070219 database of interacting proteins (Salwinski et al., 2004), with stringent criteria that exclude proteins with fewer than 50 amino acids or exhibiting $\geq 40\%$ sequence identity. The negative cases are generated by randomly pairing proteins that lack evidence of interaction, and these pairs are further filtered based on their sub-cellular locations.

Impact: The yeast dataset serves as a widely recognized benchmark (Hashemi-far et al., 2018; Yu et al., 2008) for assessing model performance, and yeast PPI prediction substantially enhances our comprehension of cellular processes by unveiling intricate protein interactions and providing crucial insights into the functional roles of proteins within yeast cells.

Human PPI prediction predicts whether two human proteins interact or not. When provided with protein sequences x_1 and x_2 from humans, the predictor generates a binary label $y \in 0, 1$ to indicate the presence or absence of interaction between them. We adopt dataset from Pan et al. (2010), comprising positive protein pairs obtained from the Human Protein Reference Database (HPRD) (Peri et al., 2003) and negative protein pairs sourced from different cellular compartments with no documented interaction (Rhodes et al., 2005). To ensure data quality, self-interactions and duplicate interactions were removed, resulting in the creation of two datasets, namely "AB" and "CD." The "AB" dataset encompasses the entire dataset, while the "CD" dataset comprises selected proteins with identities below 25%. For evaluation, we exclusively employ

the "AB" split strategy in this task.

Impact: Human PPI prediction holds immense practical significance in clinical research. Notably, insights into protein interactions linked to diseases enhance our understanding of human disease mechanisms, paving the way for innovative therapeutic strategies (Rual et al., 2005; Yu et al., 2011).

SHS PPI prediction is to classify the type of interaction between a given protein pair. Given two protein sequences, x_1 and x_2 , the model aims to predict a label y where $y \in \{0, 1, \dots, 6\}$. These interaction types encompass categories such as "reaction", "activation", "catalysis", among others. Our analysis utilizes a dataset derived from interaction pairs specific to Homo sapiens, sourced from the STRING database (Szklarczyk et al., 2016). We adopt preprocess strategies as recommended by Chen et al. (2019) where the SHS dataset is divided into two subsets: "SHS27k" and "SHS148k". For computational efficiency, our study focuses solely on the "SHS27k" subset. The data is partitioned into training, validation, and test sets at a random split ratio of 8:1:1.

Impact: Understanding and categorizing the precise interactions between protein pairs is pivotal in unraveling intricate cellular mechanisms and shedding light on complex biological pathways. This knowledge not only aids in defining drug efficacy through network-based "drug-disease proximity measures" (Guney et al., 2016) but also plays a crucial role in interpreting the outcomes of genome-wide association screens (Hillenmeyer et al., 2016).

4.3. Localization Prediction

Identifying the localization or local-related biological mechanism of proteins within various cellular compartments is of paramount importance in the process of functional annotation.

Subcellular localization prediction aims to dig out the specific cellular location of a given natural protein. Given a protein sequence denoted as x , the model assigns it to multiple possible localizations $y \in 0, 1, \dots, 9$, which may include designations such as "Nucleus" and "Cytoplasm", among others. To accomplish this task, we utilize two datasets from DeepLoc-1 (Alma-

gro Armenteros et al., 2017) and DeepLoc-2 (Thumuluri et al., 2022). For the DeepLoc-1 dataset, we apply the split methodology introduced by Stärk et al. (2021). Regarding the DeepLoc-2 dataset, its original split strategy involves 5-fold cross-validation. In our implementation, we employ the first three partitions as training data, the fourth as validation data, and ultimately evaluate the model’s performance on the SwissProt localization dataset and the human protein atlas (Thul et al., 2017).

Impact: The subcellular localization of proteins plays a crucial role in deciphering the fundamental mechanisms of diseases linked to abnormal subcellular localization (Delmolino et al., 2001; Millar et al., 2009). Notably, some proteins are recognized for their ability to localize within multiple cellular compartments, underscoring the intricate and pertinent nature of this research domain.

Binary localization prediction constitutes a sub-problem of the aforementioned task. The model’s responsibility is to decide whether a given protein x should be categorized as "membrane-bound" or "soluble," denoted as $y \in \{0, 1\}$. The datasets for training and testing are drawn from DeepLoc-1 (Almagro Armenteros et al., 2017), which includes an additional label system where "S" represents soluble, "M" corresponds to membrane-bound, and "U" signifies unknown localization. To train the model, we employ the same data partitioning method as introduced by Stärk et al. (2021), while excluding data points labeled as "U".

Impact: Predicting protein localization as either membrane-bound or soluble is vital for deciphering cellular functions, particularly in signal transduction and transport (Gimpelev et al., 2004). It plays a pivotal role in drug discovery, enabling the design of targeted therapies against membrane proteins.

Sorting signal prediction elucidates the intricate process of subcellular localization by identifying biological mechanisms within sorting signal sequences that guide proteins to specific subcellular structures or organelles. When presented with a short sequence x , the model assigns it to one of nine classes denoted as $y \in \{0, 1, \dots, 8\}$, encompassing designations such as "Signal Peptide (SP)" and "Mitochondrial Transit Peptide (MT)", among others. This consti-

tutes a multi-label classification task, and we employ the dataset sourced from DeepLoc-2 (Thumuluri et al., 2022). As the original dataset lacks an official split strategy, we perform a random split with a train/validation/test ratio of 8:1:1.

Impact: Protein sorting signals facilitate the precise intracellular localization of proteins, thereby sustaining cellular homeostasis and the integrity of subcellular compartments (Kanner et al., 2003; Nielsen et al., 2019). These signals typically entail interactions with partner proteins or sorting complexes, it is significant to investigate protein sorting signals for comprehending the intracellular localization and functional intricacies of proteins.

4.4. Solubility Prediction

This group of tasks is to predict the protein solubility, which is critical for optimizing protein expression, purification, and drug development processes.

Binary solubility prediction aims to determine whether a protein is soluble or insoluble. When presented with a protein denoted as x , the model assigns it to a binary label, $y \in \{0, 1\}$. The dataset and data partitioning approach are drawn from DeepSol (Khurana et al., 2018), where protein sequences exhibiting a sequence identity of $\geq 30\%$ to any sequence in the test set are excluded from the training set. This task shares similarities with binary localization prediction but explicitly focuses on modeling solubility.

Impact: Protein solubility is pivotal for swiftly and efficiently selecting appropriate protein samples, saving resources and time, particularly in biotechnology, drug development, and laboratory protein purification (Davis et al., 1999; Trainor et al., 2017). It improves experiment success rates and resource allocation while advancing scientific research.

E.coli solubility prediction involves forecasting the solubility value of E. coli proteins using an ensemble database, downloadable from the eSOL website (Niwa et al., 2009). When provided with a sequence from E. coli, the model predicts a regression value, denoted as $y \in \mathbb{R}$. Solubility, in this context, is defined as the ratio of the supernatant fraction to the total fraction, as determined

in physiochemical experiments referred to as PURE (Shimizu et al., 2005). We utilize the training and validation datasets sourced from GraphSol (Chen et al., 2021) and further partition the validation dataset into separate validation and test sets.

Impact: E. coli, as a prevalent host organism for protein expression, demands precise solubility predictions to optimize recombinant protein production, purification, and subsequent functional studies (Costa et al., 2014). Such predictions, based on experimental data and computational models, facilitate the selection of suitable protein candidates for diverse applications (Hebditch et al., 2017), ranging from structural biology to drug discovery and industrial processes.

Mutation solubility prediction measures the impact of mutations on protein solubility. Given a mutated protein sequence denoted as x , the model predicts the solubility change $y \in \mathbb{R}$ relative to the wild-type sequence. This task encompasses three distinct protein mutation datasets, with mutations occurring at single points within proteins such as "Beta-lactamase TEM (blat)", "Chalcone Synthase (cs)" and "Levoglucosan Kinase (lgk)". These datasets were sourced from SoluProtMutDB (Velecký et al., 2022) which provides manually curated and reliable data in the standardized format. Data points where recorded mutations did not align with the original sequence were excluded, and the training, validation, and test datasets were partitioned in an 8:1:1 ratio.

Impact: Low protein solubility is a significant hurdle in industrial processes and is implicated in numerous human diseases (Musil et al., 2018). Investigating the impact of mutations on protein solubility not only sheds light on the mechanisms underpinning disease development but also enhances the application of protein engineering in various industrial domains.

4.5. Structure Prediction

While AlphaFold (Jumper et al., 2021) and RoseTTAFold (Baek et al., 2021) have made significant strides in structure prediction, the structure prediction related task still is a rigorous assessment to evaluate the representation quality of the sequence model.

Fold prediction is the automated classification of protein sequences into one of 1,195 known protein folds, facilitating the modeling of the sequence-structure relationship. Given any sequence x , the objective is to predict the fold label $y \in 0, 1, \dots, 1194$, determined by the backbone coordinates of the corresponding protein structure. This task utilizes the dataset from Hou et al. (2018), originally derived from the SCOP 1.75 database (Fox et al., 2014). Notably, this dataset meticulously addresses homologous sequence redundancy between test and training datasets through two distinct strategies: a three-level redundancy reduction at fold/superfamily/family levels and sequence identity reduction.

Impact: Fold prediction is essential for unraveling the intricate relationship between a protein’s primary sequence and its three-dimensional structure, with profound implications for fields ranging from structural biology to drug design (Chen et al., 2016).

5. Experiments

5.1. Experimental Setups

We perform the pre-training of our models on 8 A100-80GB GPUs, using a data-parallel distribution strategy. The global batch size is set to 1024 (local batch size is set to 32), and the maximum sequence length is constrained to 1024 tokens. We employ dropout regularization with a rate of 0.1 during the pre-training phase to mitigate overfitting. The architecture comprises 12 encoder layers, with each layer having a hidden size of 768 and an intermediate size of 3072. The multi-head attention mechanism contains 12 heads, each with a dimensionality of 64. For model optimization, we utilize the Adam optimizer, with a learning rate initialized at $1e-4$. The maximum number of training steps is set to 530,000. The learning rate schedule involves a warm-up mechanism for the first 2000 iterations, following which the learning rate is linearly decayed to zero. The Adam hyperparameters are configured as follows: epsilon is $1e-8$, $\beta_1 = 0.9$ and $\beta_2 = 0.98$. Gradient clipping is applied with a maximum value of

Tokenization	BPE							
Vocab size	50	100	200	400	800	1600	3200	
Perplexity	9.51	13.66	23.67	34.87	49.64	72.39	105.01	
Normalized Perplexity	1.05	1.03	1.02	1.01	1.00	1.00	1.00	

Table 2: Perplexity and Normalized Perplexity on the validation set for the BPE model.

Tokenization	Unigram							
Vocab size	50	100	200	400	800	1600	3200	
Perplexity	8.26	12.95	26.98	62.39	81.11	115.90	220.77	
Normalized Perplexity	1.04	1.03	1.02	1.01	1.01	1.00	1.00	

Table 3: Perplexity and Normalized Perplexity on the validation set for the Unigram model.

5.0 to prevent exploding gradients. Our implementation leverages the PyTorch framework in conjunction with the Hugging Face library, aligning with best practices for efficient and scalable training of language models.

In the case of supervised tasks, all pre-trained model weights are kept fixed to ensure a fair evaluation of their representation capabilities. Classifiers are trained using a batch size of 256, a learning rate of 0.001, and the Adam optimizer. Early stopping is employed with a patience threshold of 20 epochs, with a maximum of 100 epochs for training. It’s important to note that these hyper-parameters were adopted without adjustments, drawing reference from Dallago et al. (2021). Each individual experiment underwent training three times using different random seeds, and the final results represent the average scores obtained.

5.2. Pre-training Results

Following the pre-training phase, all models achieved a reduction in loss to an acceptable level, demonstrating effective learning from the training data. Table 2 and Table 3 present the perplexity and normalized perplexity metrics

Vocab	Fitness					PPI			Localization			Solubility			Structure
	GB1	AAV	Thermo	Flu	Sta	Yeast	Human	SHS	Sub	BinLoc	Sig	BinSol	Esol	Solmut	Fold
50	4/5	2/7	2/3	1/1	1/1	1/1	1/1	1/1	3/3	1/1	1/1	1/1	0/1	3/3	0/3
100	5/5	0/7	2/3	0/1	1/1	1/1	0/1	1/1	3/3	1/1	1/1	1/1	0/1	3/3	0/3
200	4/5	2/7	2/3	1/1	0/1	1/1	1/1	1/1	3/3	1/1	1/1	1/1	0/1	3/3	0/3
800	2/5	0/7	2/3	1/1	0/1	1/1	1/1	1/1	3/3	0/1	0/1	1/1	0/1	3/3	0/3
1600	2/5	0/7	2/3	1/1	0/1	1/1	0/1	1/1	3/3	0/1	0/1	1/1	0/1	3/3	0/3
3200	2/5	0/7	2/3	1/1	0/1	1/1	0/1	1/1	3/3	0/1	0/1	1/1	0/1	3/3	0/3

Table 4: Average results on all experimental sets of each benchmark dataset. The denominator represents the number of data sets in this experiment, and the numerator represents the number of results that exceed the amino acid segmentation in this vocabulary size setting.

calculated on the test set for both Byte Pair Encoding (BPE) and Unigram models, respectively. For the base model employing a per-amino-acid (Per-AA) tokenization strategy, the *Perplexity* value is 7.78, and the corresponding *Normalized Perplexity* is 1.06.

In the supplementary materials, Figures S1 to S30 show the loss curves, as well as the perplexity and normalized perplexity curves for the pre-trained models. It is important to note that evaluations were performed at intervals of 10,000 steps. These figures collectively demonstrate that all models have converged to a reasonable range, substantiating their effectiveness in learning the underlying data distribution.

5.3. Benchmark Results Overview

To provide researchers with insights into how the augmentation of vocabulary size in Protein Language Models (PLMs) affects embedding quality, we conducted a systematic investigation. The scores in Table 4 represent the average performance of models that utilize sub-word tokenization to expand their vocabulary. Specifically, for a given vocabulary size, it indicates how many datasets, on average, surpassed the traditional Per-AA method (with a vocabulary size of 33). This is calculated as the ratio of the number of datasets where the expanded vocabulary models outperformed the Per-AA baseline to the total number of datasets across various tasks. For models with expanded vo-

cabularies, the average score on each dataset was computed from the mean of 12 experiment results (2 tokenization methods x 2 classification heads x 3 random seeds). For the baseline models, the average score on each dataset was derived from the mean of 6 experiments (2 classification heads x 3 random seeds). More detailed results of each experimental setting can be found in the supplementary materials Table S1 to S54.

Our experimental findings led to several key insights:

- **Significant Impact of Vocabulary Size.** Extensive experimentation has unequivocally demonstrated that vocabulary size profoundly influences protein representation, albeit with varying degrees of impact across different types of downstream tasks. Notably, in every dataset associated with structure prediction, an inverse relationship was observed wherein enhancements in vocabulary size correlated with negative optimization.
- **Existence of an Optimal Vocabulary Threshold.** Contrasting with language models utilized in NLP, PLMs with an excessively large vocabulary size can potentially exert detrimental effects on downstream tasks. Specifically, when the vocabulary size surpasses 800, the majority of tasks are performed suboptimally compared to the baseline model that employs per-amino-acid segmentation.

5.4. Downstream Tasks

Fitness Prediction. Table 5 showcases results for five distinct tasks under the umbrella of **Fitness Prediction** and the evaluation metrics is *Spearman correlation*. It’s worth highlighting that the datasets for **GB1**, **AAV**, and **Thermo** are multifaceted and are elaborated upon in Fig 3. A discerning observation from the data is the dichotomous impact of vocabulary augmentation. Most tasks witnessed an upswing in their performance metrics with an expanded vocabulary. However, **AAV** stood out as an anomaly, showing a marked deterioration in performance across all its datasets as the vocabulary size expanded, the maximum decrease was 21%, and the minimum decrease was

Vocab	Fitness Prediction					Localization Prediction				
	GB1*	AAV*	Thermo*	Flu	Sta	Sub-1	BinLoc	Sub-2	Sub-hpa	Sig
33	0.486	0.348	0.613	0.393	0.513	0.951	0.913	0.927	0.890	0.957
50	0.503	0.318	0.618	0.399	0.530	0.948	0.917	0.926	0.891	0.961
100	0.534	0.313	0.621	0.383	0.516	0.947	0.913	0.923	0.890	0.959
200	0.504	0.306	0.616	0.420	0.495	0.945	0.913	0.922	0.894	0.959
800	0.462	0.288	0.606	0.415	0.464	0.944	0.909	0.921	0.894	0.956
1600	0.465	0.274	0.613	0.438	0.432	0.944	0.905	0.921	0.892	0.956
3200	0.469	0.299	0.608	0.430	0.445	0.943	0.909	0.921	0.890	0.956

Table 5: Performance on **Fitness Prediction** and **Localization Prediction**. Each value indicates the average score across all experiments, maintaining a consistent vocabulary size. The averaging method is consistent with that in Section 5.2. Datasets marked with * indicate that averages were also taken across multiple data partitioning methods. For instance, **GB1** encompasses five different data segmentation methods within the same dataset. The score with a vocabulary size of 50 reflects results across 60 experimental setups ($5 \times 2 \times 2 \times 3$, representing the number of data splits, tokenization methods, classification heads, number of random seed experiments).

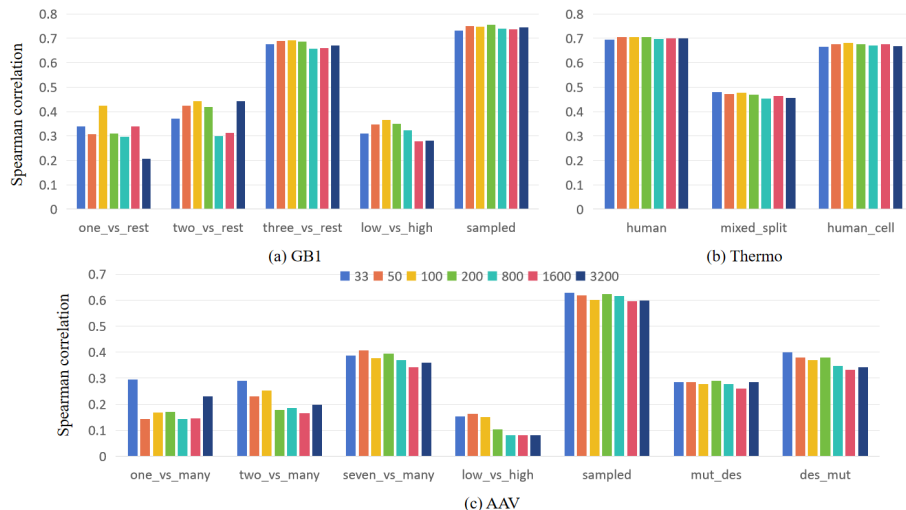


Figure 3: A detailed elaboration of the performance results for the **GB1**, **Thermo**, and **AAV** tasks across different vocabulary sizes is provided.

8.6%. In contrast, the performance of **Flu** benefited from an enlarged vocabulary. Intriguingly, the average performance for **GB1** and **Stab** began to wane after hitting a vocabulary size of 200, even underperforming the baseline model set at a vocabulary size of 33, which notably lacked any word segmentation methodologies. **Thermo** is not sensitive to vocabulary size changes, fluctuating approximately 1% up or down.

Localization Prediction. The right side of Table 5 presents results from five datasets under the category of **Localization Prediction**, and the monitor metrics is *Accuracy*. Across all datasets and partitioning methodologies, the task of subcellular localization prediction consistently achieves a remarkable classification accuracy exceeding 0.9. This accuracy remains predominantly stable, all performance fluctuations are within 1% with variations in vocabulary size. Drawing from these experimental insights, it’s evident that language models find both multi-class and single-class prediction tasks for protein localization relatively straightforward. Moreover, the vocabulary size seems to have minimal

Vocab	PPI Prediction			Solubility Prediction			Structure Prediction		
	Yeast	SHS27k	Human	Esol	BinSol	Solmut*	superfamily	family	fold
33	0.699	0.519	0.927	0.044	0.913	0.187	0.518	0.930	0.269
50	0.725	0.526	0.930	0.045	0.917	0.217	0.505	0.929	0.268
100	0.720	0.520	0.925	0.048	0.913	0.208	0.437	0.919	0.226
200	0.728	0.535	0.929	0.047	0.913	0.201	0.439	0.915	0.264
800	0.720	0.534	0.928	0.046	0.909	0.210	0.435	0.894	0.240
1600	0.733	0.531	0.925	0.048	0.905	0.213	0.418	0.890	0.231
3200	0.724	0.520	0.922	0.047	0.909	0.197	0.406	0.880	0.233

Table 7: Performance on **PPI Prediction**, **Solubility Prediction** and **Structure Prediction**. Each value indicates the average score across all experiments, maintaining a consistent vocabulary size. The averaging method is consistent with that in Section 5.2. Datasets marked with * indicate that averages were also taken across multiple data partitioning methods.

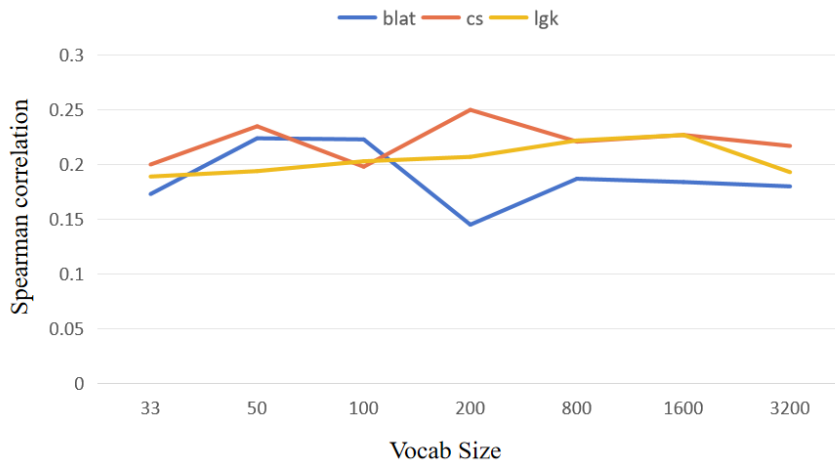


Figure 4: A detailed exposition is provided on the performance results of three distinct protein solubility mutation datasets: **Beta-lactamase TEM (blat)**, **Chalcone Synthase (cs)**, and **Levoglucozan Kinase (lgk)** across varying vocabulary sizes.

influence on the prediction outcomes for protein localization tasks.

Protein-Protein interaction Prediction. Table 7 summaries the 3 datasets from **PPI Prediction**, and the metrics is *Accuracy*. From the table, it’s readily apparent that when dealing with protein pairing tasks, more discrete tokens are beneficial for distinguishing the relationships between protein pairs. Additionally, datasets that are harder to classify witness higher performance enhancements. For instance, in the **Yeast** dataset, the model with a vocabulary size of 1600 exhibited a 5% average score increase compared to the model with a vocabulary size of 33. In **SHS27k**, every increase in vocabulary size resulted in performance improvements, with a peak boost of 3%. In contrast, while the **Human** dataset showed improvements across the board, the maximum increase was a mere 0.4%.

Solubility Prediction. The central section of Table 7 displays the findings for **Solubility Prediction**. While the evaluation metric for the three datasets in Solmut is the *Spearman correlation*, **Esol** employs *MSE*, **BinSol** and **DeepSol** use *Accuracy* as their metric. Predicting solubility regression values for **Esol** proves to be relatively straightforward, given the lower MSE scores and models of varying vocabulary sizes exhibit almost uniform predictive capabilities. **BinSol** observed a similar situation to **Esol**, the numerical fluctuations of results are less than 1%. An analysis of the **Solmut** datasets indicates that models with expanded vocabulary sizes have the potential to improve performance by 20% to 30% as shown in Fig 4. Although most instances show enhancement, occasional instability is detected. Such variability could be attributed to the alterations in the inherent characteristics of proteins post-mutation.

Structure Prediction. The results for **Structure Prediction** are detailed on the right side of Table 7, and the metrics is *Accuracy*. In the context of fold prediction, a notable trend emerges: as the vocabulary size enlarges, there is a pronounced decrease in performance across all datasets. To illustrate, the **superfamily** category registers the most significant drop, plummeting by 21.6%, while the **family** and **fold** categories experience declines of 5.3% and 16% respectively. This pattern underscores a consistent downturn in performance correlating with the augmentation of the vocabulary size. Such regression

Vocab	BPE					Unigram				
	Fit	PPI	Loc	Sol	Stru	Fit	PPI	Loc	Sol	Stru
50	0.470	0.722	0.934	0.456	0.558	0.477	0.731	0.933	0.453	0.576
100	0.471	0.721	0.932	0.446	0.534	0.476	0.722	0.930	0.458	0.521
200	0.474	0.731	0.932	0.454	0.549	0.462	0.731	0.931	0.449	0.530
800	0.454	0.728	0.930	0.456	0.523	0.441	0.726	0.928	0.456	0.523
1600	0.452	0.732	0.929	0.457	0.515	0.437	0.727	0.927	0.459	0.510
3200	0.452	0.723	0.928	0.443	0.509	0.448	0.722	0.929	0.453	0.504

Table 8: The average results of different downstream task groups under the same vocabulary with varying tokenization methods are presented. Each score represents the average score of all experiments within that task group, encompassing different tasks, datasets, classification heads, and random seeds.

may stem from the amalgamation of multiple amino acid tokens in the encoding process, possibly veiling intricate local structural nuances. As a result, the surge in diversity might be detrimentally affecting the classification efficacy.

5.5. Ablation Study

Analysis of tokenizers. From Table 8, it can be observed that the discrepancies arising from different tokenization methods are minimal across various downstream tasks. The main source of performance variation stems from the impact of vocabulary size on model representation. Across different tasks, as the vocabulary size increases, the model performance exhibits a bell-shaped curve, showing an initial increase followed by a decline.

Impact of pooling heads. From Table 9, it can be observed that, when freezing the pre-trained model parameters and only tuning the pooling head, the performance is highly correlated with the choice of the classification head. When using the same vocabulary size, the attention1d pooling method outperforms the mean pooling method. Additionally, similar to the results in Table 8, as the vocabulary size increases, the model’s representational capacity across various downstream tasks tends to decline.

Vocab	Mean Pooling					Attention1d Pooling				
	Fit	PPI	Loc	Sol	Stru	Fit	PPI	Loc	Sol	Stru
50	0.411	0.706	0.930	0.418	0.562	0.537	0.748	0.937	0.490	0.572
100	0.415	0.701	0.924	0.420	0.526	0.531	0.742	0.938	0.484	0.529
200	0.412	0.708	0.925	0.427	0.543	0.524	0.753	0.937	0.476	0.536
800	0.393	0.700	0.922	0.429	0.520	0.501	0.755	0.936	0.483	0.526
1600	0.392	0.697	0.920	0.432	0.514	0.497	0.761	0.936	0.484	0.512
3200	0.398	0.687	0.921	0.415	0.506	0.502	0.757	0.936	0.481	0.507

Table 9: The average results of different downstream task groups under the same vocabulary with varying pooling heads are presented. Each score represents the average score of all experiments within that task group, encompassing different tasks, datasets, classification heads, and random seeds.

6. Conclusion

In this paper, we introduce PETA, a vocabulary study optimized for protein language models across a broad range of datasets. To mitigate potential biases arising from different tokenization methods, classification heads, and random seeds, for each fixed vocabulary size, we employed both BPE and Unigram tokenization methods, two classification heads (mean pooling and attention1d pooling), and experiments with three different random seeds on each dataset. Ultimately, we found that expanding the vocabulary size to some extent (50-200) generally enhances performance on downstream tasks. However, once the vocabulary size surpasses 800, the model’s representational power exhibits a broad decline across most tasks. We hope that this work and benchmark will influence the future protein language model community and contribute positively to human health, environmental development, and biomedicine.

CRedit authorship contribution statement

Yang Tan: Conceptualization of this study, Methodology, Data curation, Implementation, writing & editing. Mingchen Li: Conceptualization of this

study, Methodology, Data curation, Implementation, writing & editing. Pan Tan: Review & editing. Ziyi Zhou: Review & editing. Huiqun Yu: Supervision, review & editing. Guisheng Fan: Supervision, review & editing. Liang Hong: Supervision, review & editing.

Declaration of competing interest

The authors declare that they have no known competing financial interests or personal relationships that could have appeared to influence the work reported in this paper.

Data availability

Data released on GitHub. <https://github.com/ginnm/ProteinPretraining>

References

- Alley, E. C., Khimulya, G., Biswas, S., AlQuraishi, M., & Church, G. M. (2019). Unified rational protein engineering with sequence-based deep representation learning. *Nature methods*, *16*, 1315–1322.
- Almagro Armenteros, J. J., Sønderby, C. K., Sønderby, S. K., Nielsen, H., & Winther, O. (2017). Deeploc: Prediction of protein subcellular localization using deep learning. *Bioinformatics*, *33*, 3387–3395.
- Arnold, F. H. (1998). Design by directed evolution. *Accounts of chemical research*, *31*, 125–131.
- Asgari, E., McHardy, A. C., & Mofrad, M. R. (2019). Probabilistic variable-length segmentation of protein sequences for discriminative motif discovery (dimotif) and sequence embedding (protvecx). *Scientific reports*, *9*, 3577.
- Baek, M., DiMaio, F., Anishchenko, I., Dauparas, J., Ovchinnikov, S., Lee, G. R., Wang, J., Cong, Q., Kinch, L. N., Schaeffer, R. D. et al. (2021).

Accurate prediction of protein structures and interactions using a three-track neural network. *Science*, 373, 871–876.

Bengio, Y., Ducharme, R., & Vincent, P. (2000). A neural probabilistic language model. *Advances in neural information processing systems*, 13.

Berman, H. M., Westbrook, J., Feng, Z., Gilliland, G., Bhat, T. N., Weissig, H., Shindyalov, I. N., & Bourne, P. E. (2000). The protein data bank. *Nucleic acids research*, 28, 235–242.

Biswas, S., Khimulya, G., Alley, E. C., Esvelt, K. M., & Church, G. M. (2021). Low-n protein engineering with data-efficient deep learning. *Nature methods*, 18, 389–396.

Bryant, D. H., Bashir, A., Sinai, S., Jain, N. K., Ogden, P. J., Riley, P. F., Church, G. M., Colwell, L. J., & Kelsic, E. D. (2021). Deep diversification of an aav capsid protein by machine learning. *Nature Biotechnology*, 39, 691–696.

Capel, H., Weiler, R., Dijkstra, M., Vleugels, R., Bloem, P., & Feenstra, K. A. (2022). Proteinglue multi-task benchmark suite for self-supervised protein modeling. *Scientific Reports*, 12, 16047.

Chen, B., Cheng, X., Geng, Y.-a., Li, S., Zeng, X., Wang, B., Gong, J., Liu, C., Zeng, A., Dong, Y. et al. (2023). Xtrimopglm: Unified 100b-scale pre-trained transformer for deciphering the language of protein. *bioRxiv*, (pp. 2023–07).

Chen, D., Tian, X., Zhou, B., Gao, J. et al. (2016). Profold: Protein fold classification with additional structural features and a novel ensemble classifier. *BioMed research international*, 2016.

Chen, J., Zheng, S., Zhao, H., & Yang, Y. (2021). Structure-aware protein solubility prediction from sequence through graph convolutional network and predicted contact map. *Journal of cheminformatics*, 13, 1–10.

- Chen, M., Ju, C. J.-T., Zhou, G., Chen, X., Zhang, T., Chang, K.-W., Zaniolo, C., & Wang, W. (2019). Multifaceted protein-protein interaction prediction based on siamese residual rcnn. *Bioinformatics*, *35*, i305–i314.
- Choo, S., & Kim, W. (2023). A study on the evaluation of tokenizer performance in natural language processing. *Applied Artificial Intelligence*, *37*, 2175112.
- Consortium, U. (2019). Uniprot: A worldwide hub of protein knowledge. *Nucleic acids research*, *47*, D506–D515.
- Costa, S., Almeida, A., Castro, A., & Domingues, L. (2014). Fusion tags for protein solubility, purification and immunogenicity in escherichia coli: The novel fh8 system. *Frontiers in microbiology*, *5*, 63.
- Dallago, C., Mou, J., Johnston, K. E., Wittmann, B. J., Bhattacharya, N., Goldman, S., Madani, A., & Yang, K. K. (2021). Flip: Benchmark tasks in fitness landscape inference for proteins. *bioRxiv*, (pp. 2021–11).
- Dauparas, J., Anishchenko, I., Bennett, N., Bai, H., Ragotte, R. J., Milles, L. F., Wicky, B. I., Courbet, A., de Haas, R. J., Bethel, N. et al. (2022). Robust deep learning-based protein sequence design using proteinmpnn. *Science*, *378*, 49–56.
- Davis, G. D., Elisee, C., Newham, D. M., & Harrison, R. G. (1999). New fusion protein systems designed to give soluble expression in escherichia coli. *Biotechnology and bioengineering*, *65*, 382–388.
- Delmolino, L. M., Saha, P., & Dutta, A. (2001). Multiple mechanisms regulate subcellular localization of human cdc6. *Journal of Biological Chemistry*, *276*, 26947–26954.
- Deng, J., Dong, W., Socher, R., Li, L.-J., Li, K., & Fei-Fei, L. (2009). Imagenet: A large-scale hierarchical image database. In *2009 IEEE conference on computer vision and pattern recognition* (pp. 248–255). Ieee.

- Devlin, J., Chang, M.-W., Lee, K., & Toutanova, K. (2018). Bert: Pre-training of deep bidirectional transformers for language understanding. *arXiv preprint arXiv:1810.04805*, .
- Doudna, J. A., & Charpentier, E. (2014). The new frontier of genome engineering with crispr-cas9. *Science*, *346*, 1258096.
- Du, Z., Qian, Y., Liu, X., Ding, M., Qiu, J., Yang, Z., & Tang, J. (2021). Glm: General language model pretraining with autoregressive blank infilling. *arXiv preprint arXiv:2103.10360*, .
- Elnaggar, A., Essam, H., Salah-Eldin, W., Moustafa, W., Elkerdawy, M., Rochereau, C., & Rost, B. (2023). Ankh: Optimized protein language model unlocks general-purpose modelling. *bioRxiv*, (pp. 2023–01).
- Elnaggar, A., Heinzinger, M., Dallago, C., Rehawi, G., Wang, Y., Jones, L., Gibbs, T., Feher, T., Angerer, C., Steinegger, M. et al. (2021). Prottrans: Toward understanding the language of life through self-supervised learning. *IEEE transactions on pattern analysis and machine intelligence*, *44*, 7112–7127.
- Feng, Y., De Franceschi, G., Kahraman, A., Soste, M., Melnik, A., Boersema, P. J., De Laureto, P. P., Nikolaev, Y., Oliveira, A. P., & Picotti, P. (2014). Global analysis of protein structural changes in complex proteomes. *Nature biotechnology*, *32*, 1036–1044.
- Ferruz, N., Schmidt, S., & Höcker, B. (2022). Protgpt2 is a deep unsupervised language model for protein design. *Nature communications*, *13*, 4348.
- Fowler, D. M., & Fields, S. (2014). Deep mutational scanning: a new style of protein science. *Nature methods*, *11*, 801–807.
- Fox, N. K., Brenner, S. E., & Chandonia, J.-M. (2014). Scope: Structural classification of proteins—extended, integrating scop and astral data and classification of new structures. *Nucleic acids research*, *42*, D304–D309.

- Gage, P. (1994). A new algorithm for data compression. *C Users Journal*, *12*, 23–38.
- Gimpelev, M., Forrest, L. R., Murray, D., & Honig, B. (2004). Helical packing patterns in membrane and soluble proteins. *Biophysical journal*, *87*, 4075–4086.
- Girod, A., Wobus, C. E., Zádori, Z., Ried, M., Leike, K., Tijssen, P., Kleinschmidt, J. A., & Hallek, M. (2002). The vp1 capsid protein of adeno-associated virus type 2 is carrying a phospholipase a2 domain required for virus infectivity. *Journal of General Virology*, *83*, 973–978.
- Gray, V. E., Hause, R. J., Luebeck, J., Shendure, J., & Fowler, D. M. (2018). Quantitative missense variant effect prediction using large-scale mutagenesis data. *Cell systems*, *6*, 116–124.
- Guney, E., Menche, J., Vidal, M., & Barábasi, A.-L. (2016). Network-based in silico drug efficacy screening. *Nature communications*, *7*, 10331.
- Guo, Y., Yu, L., Wen, Z., & Li, M. (2008). Using support vector machine combined with auto covariance to predict protein-protein interactions from protein sequences. *Nucleic acids research*, *36*, 3025–3030.
- Haki, G., & Rakshit, S. (2003). Developments in industrially important thermostable enzymes: a review. *Bioresource technology*, *89*, 17–34.
- Hashemifar, S., Neyshabur, B., Khan, A. A., & Xu, J. (2018). Predicting protein-protein interactions through sequence-based deep learning. *Bioinformatics*, *34*, i802–i810.
- Hebditch, M., Carballo-Amador, M. A., Charonis, S., Curtis, R., & Warwicker, J. (2017). Protein-sol: A web tool for predicting protein solubility from sequence. *Bioinformatics*, *33*, 3098–3100.
- Hillenmeyer, S., Davis, L. K., Gamazon, E. R., Cook, E. H., Cox, N. J., & Altman, R. B. (2016). Stams: String-assisted module search for genome

- wide association studies and application to autism. *Bioinformatics*, *32*, 3815–3822.
- Hou, J., Adhikari, B., & Cheng, J. (2018). DeepSF: Deep convolutional neural network for mapping protein sequences to folds. *Bioinformatics*, *34*, 1295–1303.
- Hsu, C., Verkuil, R., Liu, J., Lin, Z., Hie, B., Sercu, T., Lerer, A., & Rives, A. (2022). Learning inverse folding from millions of predicted structures. In *International Conference on Machine Learning* (pp. 8946–8970). PMLR.
- Hsu, P. D., Lander, E. S., & Zhang, F. (2014). Development and applications of CRISPR-Cas9 for genome engineering. *Cell*, *157*, 1262–1278.
- Huang, K., Fu, T., Gao, W., Zhao, Y., Roohani, Y., Leskovec, J., Coley, C. W., Xiao, C., Sun, J., & Zitnik, M. (2021). Therapeutics data commons: Machine learning datasets and tasks for drug discovery and development. *arXiv preprint arXiv:2102.09548*, .
- Jarzab, A., Kurzawa, N., Hopf, T., Moerch, M., Zecha, J., Leijten, N., Bian, Y., Musiol, E., Maschberger, M., Stoeckl, G. et al. (2020). Meltome atlas—thermal proteome stability across the tree of life. *Nature methods*, *17*, 495–503.
- Jing, B., Eismann, S., Suriana, P., Townshend, R. J., & Dror, R. (2020). Learning from protein structure with geometric vector perceptrons. *arXiv preprint arXiv:2009.01411*, .
- Joo, H., Lin, Z., & Arnold, F. H. (1999). Laboratory evolution of peroxide-mediated cytochrome p450 hydroxylation. *Nature*, *399*, 670–673.
- Jumper, J., Evans, R., Pritzel, A., Green, T., Figurnov, M., Ronneberger, O., Tunyasuvunakool, K., Bates, R., Žídek, A., Potapenko, A. et al. (2021). Highly accurate protein structure prediction with AlphaFold. *Nature*, *596*, 583–589.

- Kanner, E. M., Friedlander, M., & Simon, S. M. (2003). Co-translational targeting and translocation of the amino terminus of opsin across the endoplasmic membrane requires gtp but not atp. *Journal of Biological Chemistry*, *278*, 7920–7926.
- Kay, W., Carreira, J., Simonyan, K., Zhang, B., Hillier, C., Vijayanarasimhan, S., Viola, F., Green, T., Back, T., Natsev, P. et al. (2017). The kinetics human action video dataset. *arXiv preprint arXiv:1705.06950*, .
- Khurana, S., Rawi, R., Kunji, K., Chuang, G.-Y., Bensmail, H., & Mall, R. (2018). Deepsol: A deep learning framework for sequence-based protein solubility prediction. *Bioinformatics*, *34*, 2605–2613.
- Kryshtafovych, A., Schwede, T., Topf, M., Fidelis, K., & Moult, J. (2021). Critical assessment of methods of protein structure prediction (casp)—round xiv. *Proteins: Structure, Function, and Bioinformatics*, *89*, 1607–1617.
- Labas, Y. A., Gurskaya, N., Yanushevich, Y. G., Fradkov, A., Lukyanov, K., Lukyanov, S., & Matz, M. (2002). Diversity and evolution of the green fluorescent protein family. *Proceedings of the National Academy of Sciences*, *99*, 4256–4261.
- Lan, Z., Chen, M., Goodman, S., Gimpel, K., Sharma, P., & Soricut, R. (2019). Albert: A lite bert for self-supervised learning of language representations. *arXiv preprint arXiv:1909.11942*, .
- Le, Q., & Mikolov, T. (2014). Distributed representations of sentences and documents. In *International conference on machine learning* (pp. 1188–1196). PMLR.
- Lee, H. C. (2006). Structure and enzymatic functions of human cd38. *Molecular medicine*, *12*, 317–323.
- Lesley, S. A. (2001). High-throughput proteomics: Protein expression and purification in the postgenomic world. *Protein expression and purification*, *22*, 159–164.

- Li, M., Kang, L., Xiong, Y., Wang, Y. G., Fan, G., Tan, P., & Hong, L. (2023). Sesnet: Sequence-structure feature-integrated deep learning method for data-efficient protein engineering. *Journal of Cheminformatics*, *15*, 1–13.
- Lin, T.-Y., Maire, M., Belongie, S., Hays, J., Perona, P., Ramanan, D., Dollár, P., & Zitnick, C. L. (2014). Microsoft coco: Common objects in context. In *Computer Vision–ECCV 2014: 13th European Conference, Zurich, Switzerland, September 6–12, 2014, Proceedings, Part V 13* (pp. 740–755). Springer.
- Lin, Z., Akin, H., Rao, R., Hie, B., Zhu, Z., Lu, W., Smetanin, N., Verkuil, R., Kabeli, O., Shmueli, Y. et al. (2023). Evolutionary-scale prediction of atomic-level protein structure with a language model. *Science*, *379*, 1123–1130.
- Lu, A. X., Zhang, H., Ghassemi, M., & Moses, A. (2020). Self-supervised contrastive learning of protein representations by mutual information maximization. *BioRxiv*, (pp. 2020–09).
- Luo, Y., Jiang, G., Yu, T., Liu, Y., Vo, L., Ding, H., Su, Y., Qian, W. W., Zhao, H., & Peng, J. (2021). Ecnnet is an evolutionary context-integrated deep learning framework for protein engineering. *Nature communications*, *12*, 5743.
- Ma, B. (2015). Novor: Real-time peptide de novo sequencing software. *Journal of the American Society for Mass Spectrometry*, *26*, 1885–1894.
- Madani, A., Krause, B., Greene, E. R., Subramanian, S., Mohr, B. P., Holton, J. M., Olmos Jr, J. L., Xiong, C., Sun, Z. Z., Socher, R. et al. (2023). Large language models generate functional protein sequences across diverse families. *Nature Biotechnology*, (pp. 1–8).
- McCallister, E. L., Alm, E., & Baker, D. (2000). Critical role of β -hairpin formation in protein g folding. *Nature structural biology*, *7*, 669–673.

- Meier, J., Rao, R., Verkuil, R., Liu, J., Sercu, T., & Rives, A. (2021). Language models enable zero-shot prediction of the effects of mutations on protein function. *Advances in Neural Information Processing Systems*, *34*, 29287–29303.
- Mejía-Guerra, M. K., & Buckler, E. S. (2019). A k-mer grammar analysis to uncover maize regulatory architecture. *BMC plant biology*, *19*, 1–17.
- Mikolov, T., Sutskever, I., Chen, K., Corrado, G. S., & Dean, J. (2013). Distributed representations of words and phrases and their compositionality. *Advances in neural information processing systems*, *26*.
- Millar, A. H., Carrie, C., Pogson, B., & Whelan, J. (2009). Exploring the function-location nexus: using multiple lines of evidence in defining the subcellular location of plant proteins. *The Plant Cell*, *21*, 1625–1631.
- Moal, I. H., & Fernández-Recio, J. (2012). Skempi: A structural kinetic and energetic database of mutant protein interactions and its use in empirical models. *Bioinformatics*, *28*, 2600–2607.
- Musil, M., Konegger, H., Hon, J., Bednar, D., & Damborsky, J. (2018). Computational design of stable and soluble biocatalysts. *Acs Catalysis*, *9*, 1033–1054.
- Nielsen, H., Tsigos, K. D., Brunak, S., & von Heijne, G. (2019). A brief history of protein sorting prediction. *The protein journal*, *38*, 200–216.
- Nijkamp, E., Ruffolo, J., Weinstein, E. N., Naik, N., & Madani, A. (2022). Progen2: Exploring the boundaries of protein language models. *arXiv preprint arXiv:2206.13517*, .
- Nikam, R., Kulandaisamy, A., Harini, K., Sharma, D., & Gromiha, M. M. (2021). Prothermdb: Thermodynamic database for proteins and mutants revisited after 15 years. *Nucleic acids research*, *49*, D420–D424.

- Niwa, T., Ying, B.-W., Saito, K., Jin, W., Takada, S., Ueda, T., & Taguchi, H. (2009). Bimodal protein solubility distribution revealed by an aggregation analysis of the entire ensemble of escherichia coli proteins. *Proceedings of the National Academy of Sciences*, *106*, 4201–4206.
- Notin, P., Dias, M., Frazer, J., Hurtado, J. M., Gomez, A. N., Marks, D., & Gal, Y. (2022). Tranception: Protein fitness prediction with autoregressive transformers and inference-time retrieval. In *International Conference on Machine Learning* (pp. 16990–17017). PMLR.
- Pan, X.-Y., Zhang, Y.-N., & Shen, H.-B. (2010). Large-scale prediction of human protein-protein interactions from amino acid sequence based on latent topic features. *Journal of proteome research*, *9*, 4992–5001.
- Peri, S., Navarro, J. D., Amanchy, R., Kristiansen, T. Z., Jonnalagadda, C. K., Surendranath, V., Niranjana, V., Muthusamy, B., Gandhi, T., Gronborg, M. et al. (2003). Development of human protein reference database as an initial platform for approaching systems biology in humans. *Genome research*, *13*, 2363–2371.
- Raffel, C., Shazeer, N., Roberts, A., Lee, K., Narang, S., Matena, M., Zhou, Y., Li, W., & Liu, P. J. (2020). Exploring the limits of transfer learning with a unified text-to-text transformer. *The Journal of Machine Learning Research*, *21*, 5485–5551.
- Rao, R., Bhattacharya, N., Thomas, N., Duan, Y., Chen, P., Canny, J., Abbeel, P., & Song, Y. (2019). Evaluating protein transfer learning with tape. *Advances in neural information processing systems*, *32*.
- Rao, R. M., Liu, J., Verkuil, R., Meier, J., Canny, J., Abbeel, P., Sercu, T., & Rives, A. (2021). Msa transformer. In *International Conference on Machine Learning* (pp. 8844–8856). PMLR.
- Rhodes, D. R., Tomlins, S. A., Varambally, S., Mahavisno, V., Barrette, T., Kalyana-Sundaram, S., Ghosh, D., Pandey, A., & Chinnaiyan, A. M.

- (2005). Probabilistic model of the human protein-protein interaction network. *Nature biotechnology*, *23*, 951–959.
- Riesselman, A. J., Ingraham, J. B., & Marks, D. S. (2018). Deep generative models of genetic variation capture the effects of mutations. *Nature methods*, *15*, 816–822.
- Rives, A., Meier, J., Sercu, T., Goyal, S., Lin, Z., Liu, J., Guo, D., Ott, M., Zitnick, C. L., Ma, J. et al. (2021). Biological structure and function emerge from scaling unsupervised learning to 250 million protein sequences. *Proceedings of the National Academy of Sciences*, *118*, e2016239118.
- Rocklin, G. J., Chidyausiku, T. M., Goreshnik, I., Ford, A., Houliston, S., Lemak, A., Carter, L., Ravichandran, R., Mulligan, V. K., Chevalier, A. et al. (2017). Global analysis of protein folding using massively parallel design, synthesis, and testing. *Science*, *357*, 168–175.
- Rual, J.-F., Venkatesan, K., Hao, T., Hirozane-Kishikawa, T., Dricot, A., Li, N., Berriz, G. F., Gibbons, F. D., Dreze, M., Ayivi-Guedehoussou, N. et al. (2005). Towards a proteome-scale map of the human protein-protein interaction network. *Nature*, *437*, 1173–1178.
- Rust, P., Pfeiffer, J., Vulić, I., Ruder, S., & Gurevych, I. (2020). How good is your tokenizer? on the monolingual performance of multilingual language models. *arXiv preprint arXiv:2012.15613*, .
- Salwinski, L., Miller, C. S., Smith, A. J., Pettit, F. K., Bowie, J. U., & Eisenberg, D. (2004). The database of interacting proteins: 2004 update. *Nucleic acids research*, *32*, D449–D451.
- Sarkisyan, K. S., Bolotin, D. A., Meer, M. V., Usmanova, D. R., Mishin, A. S., Sharonov, G. V., Ivankov, D. N., Bozhanova, N. G., Baranov, M. S., Soylemez, O. et al. (2016). Local fitness landscape of the green fluorescent protein. *Nature*, *533*, 397–401.

- Sauer-Eriksson, A. E., Kleywegt, G. J., Uhlén, M., & Jones, T. A. (1995). Crystal structure of the c2 fragment of streptococcal protein g in complex with the fc domain of human igg. *Structure*, *3*, 265–278.
- Scott, D. E., Bayly, A. R., Abell, C., & Skidmore, J. (2016). Small molecules, big targets: Drug discovery faces the protein–protein interaction challenge. *Nature Reviews Drug Discovery*, *15*, 533–550.
- Sharan, R., Ulitsky, I., & Shamir, R. (2007). Network-based prediction of protein function. *Molecular systems biology*, *3*, 88.
- Shimizu, Y., Kanamori, T., & Ueda, T. (2005). Protein synthesis by pure translation systems. *Methods*, *36*, 299–304.
- Shoichet, B. K., Baase, W. A., Kuroki, R., & Matthews, B. W. (1995). A relationship between protein stability and protein function. *Proceedings of the National Academy of Sciences*, *92*, 452–456.
- Stärk, H., Dallago, C., Heinzinger, M., & Rost, B. (2021). Light attention predicts protein location from the language of life. *Bioinformatics Advances*, *1*, vbab035.
- Su, J., Lu, Y., Pan, S., Murtadha, A., Wen, B., & Liu, Y. (2021). Roformer: Enhanced transformer with rotary position embedding. *arXiv preprint arXiv:2104.09864*, .
- Suzek, B. E., Wang, Y., Huang, H., McGarvey, P. B., Wu, C. H., & Consortium, U. (2015). Uniref clusters: A comprehensive and scalable alternative for improving sequence similarity searches. *Bioinformatics*, *31*, 926–932.
- Szklarczyk, D., Morris, J. H., Cook, H., Kuhn, M., Wyder, S., Simonovic, M., Santos, A., Doncheva, N. T., Roth, A., Bork, P. et al. (2016). The string database in 2017: Quality-controlled protein-protein association networks, made broadly accessible. *Nucleic acids research*, (p. gkw937).

- Thul, P. J., Åkesson, L., Wiking, M., Mahdessian, D., Geladaki, A., Ait Blal, H., Alm, T., Asplund, A., Björk, L., Breckels, L. M. et al. (2017). A subcellular map of the human proteome. *Science*, *356*, eaal3321.
- Thumuluri, V., Almagro Armenteros, J. J., Johansen, A. R., Nielsen, H., & Winther, O. (2022). Deeploc 2.0: Multi-label subcellular localization prediction using protein language models. *Nucleic Acids Research*, *50*, W228–W234.
- Trainor, K., Broom, A., & Meiering, E. M. (2017). Exploring the relationships between protein sequence, structure and solubility. *Current opinion in structural biology*, *42*, 136–146.
- Vandenberghe, L., Wilson, J., & Gao, G. (2009). Tailoring the aav vector capsid for gene therapy. *Gene therapy*, *16*, 311–319.
- Varadi, M., Anyango, S., Deshpande, M., Nair, S., Natassia, C., Yordanova, G., Yuan, D., Stroe, O., Wood, G., Laydon, A. et al. (2022). Alphafold protein structure database: massively expanding the structural coverage of protein-sequence space with high-accuracy models. *Nucleic acids research*, *50*, D439–D444.
- Vaswani, A., Shazeer, N., Parmar, N., Uszkoreit, J., Jones, L., Gomez, A. N., Kaiser, Ł., & Polosukhin, I. (2017). Attention is all you need. *Advances in neural information processing systems*, *30*.
- Velecký, J., Hamsikova, M., Stourac, J., Musil, M., Damborsky, J., Bednar, D., & Mazurenko, S. (2022). Soluprotmutdb: A manually curated database of protein solubility changes upon mutations. *Computational and Structural Biotechnology Journal*, *20*, 6339–6347.
- Wan, F., & Zeng, J. (2016). Deep learning with feature embedding for compound-protein interaction prediction. *Biorxiv*, (p. 086033).
- Wang, A., Pruksachatkun, Y., Nangia, N., Singh, A., Michael, J., Hill, F., Levy, O., & Bowman, S. (2019). Superglue: A stickier benchmark for general-

- purpose language understanding systems. *Advances in neural information processing systems*, 32.
- Wang, A., Singh, A., Michael, J., Hill, F., Levy, O., & Bowman, S. R. (2018). Glue: A multi-task benchmark and analysis platform for natural language understanding. *arXiv preprint arXiv:1804.07461*, .
- Wang, J., Yang, B., Revote, J., Leier, A., Marquez-Lago, T. T., Webb, G., Song, J., Chou, K.-C., & Lithgow, T. (2017). Possum: A bioinformatics toolkit for generating numerical sequence feature descriptors based on pssm profiles. *Bioinformatics*, 33, 2756–2758.
- Wang, Z., Combs, S. A., Brand, R., Calvo, M. R., Xu, P., Price, G., Golovach, N., Salawu, E. O., Wise, C. J., Ponnappalli, S. P. et al. (2022). Lm-gvp: An extensible sequence and structure informed deep learning framework for protein property prediction. *Scientific reports*, 12, 6832.
- Willig, K. I., Kellner, R. R., Medda, R., Hein, B., Jakobs, S., & Hell, S. W. (2006). Nanoscale resolution in gfp-based microscopy. *Nature methods*, 3, 721–723.
- Wu, N. C., Dai, L., Olson, C. A., Lloyd-Smith, J. O., & Sun, R. (2016). Adaptation in protein fitness landscapes is facilitated by indirect paths. *Elife*, 5, e16965.
- Xu, M., Zhang, Z., Lu, J., Zhu, Z., Zhang, Y., Chang, M., Liu, R., & Tang, J. (2022). Peer: A comprehensive and multi-task benchmark for protein sequence understanding. *Advances in Neural Information Processing Systems*, 35, 35156–35173.
- Yang, K. K., Fusi, N., & Lu, A. X. (2022a). Convolutions are competitive with transformers for protein sequence pretraining. *bioRxiv*, (pp. 2022–05).
- Yang, K. K., Zanichelli, N., & Yeh, H. (2022b). Masked inverse folding with sequence transfer for protein representation learning. *bioRxiv*, (pp. 2022–05).

- Ye, H., Chen, Z., Wang, D.-H., & Davison, B. (2020). Pretrained generalized autoregressive model with adaptive probabilistic label clusters for extreme multi-label text classification. In *International Conference on Machine Learning* (pp. 10809–10819). PMLR.
- Yeoman, C. J., Han, Y., Dodd, D., Schroeder, C. M., Mackie, R. I., & Cann, I. K. (2010). Thermostable enzymes as biocatalysts in the biofuel industry. *Advances in applied microbiology*, *70*, 1–55.
- Yu, H., Braun, P., Yildirim, M. A., Lemmens, I., Venkatesan, K., Sahalie, J., Hirozane-Kishikawa, T., Gebreab, F., Li, N., Simonis, N. et al. (2008). High-quality binary protein interaction map of the yeast interactome network. *Science*, *322*, 104–110.
- Yu, H., Tardivo, L., Tam, S., Weiner, E., Gebreab, F., Fan, C., Svrikapa, N., Hirozane-Kishikawa, T., Rietman, E., Yang, X. et al. (2011). Next-generation sequencing to generate interactome datasets. *Nature methods*, *8*, 478–480.
- Zhang, Z., Xu, M., Chenthamarakshan, V., Lozano, A., Das, P., & Tang, J. (2023). Enhancing protein language models with structure-based encoder and pre-training. *arXiv preprint arXiv:2303.06275*, .
- Zhang, Z., Xu, M., Jamasb, A., Chenthamarakshan, V., Lozano, A., Das, P., & Tang, J. (2022). Protein representation learning by geometric structure pretraining. *arXiv preprint arXiv:2203.06125*, .
- Zheng, Z., Deng, Y., Xue, D., Zhou, Y., Ye, F., & Gu, Q. (2023). Structure-informed language models are protein designers. *bioRxiv*, (pp. 2023–02).
- Zhou, N., Jiang, Y., Bergquist, T. R., Lee, A. J., Kacsóh, B. Z., Crocker, A. W., Lewis, K. A., Georghiou, G., Nguyen, H. N., Hamid, M. N. et al. (2019). The cafa challenge reports improved protein function prediction and new functional annotations for hundreds of genes through experimental screens. *Genome biology*, *20*, 1–23.